Nuclear magnetic moment of ^{59}Cu with on-line β-NMR on oriented nuclei

V. V. Golovko,[1,*] I. Kraev,[1] T. Phalet,[1] N. Severijns,[1] B. Delauré,[1] M. Beck,[1] V. Kozlov,[1] A. Lindroth,[1] S. Versyck,[1] D. Zákoucký,[2] D. Vénos,[2] D. Srnka,[2] M. Honusek,[2] P. Herzog,[3] C. Tramm,[3] U. Köster,[4] and I. S. Towner[5]

[1]*Instituut voor Kern- en Stralingsfysica, Katholieke Universiteit Leuven, B-3001 Leuven, Belgium*

[2]*Nuclear Physics Institute, ASCR, 250 68 Řež, Czech Republic*

[3]*Helmholtz-Institut für Strahlen- und Kernphysik, Universität Bonn, D-53115 Bonn, Germany*

[4]*ISOLDE, CERN, CH-1211 Genève 23, Switzerland*

[5]*Physics Department, Queen's University, Kingston, Ontario, Canada K7L 3N6*

(Received 13 April 2004; published 21 July 2004)

The nuclear magnetic moment of the nucleus ^{59}Cu, with one proton and two neutrons outside the closed $N=Z=28$ shells, was measured in an on-line experiment combining β-NMR with low temperature nuclear orientation and with particle detectors operating at a temperature of about 10 K. From the data the center frequency $\nu(B_{ext}=0)=209.51(22)$ MHz was derived. Using the hyperfine field of Cu in host iron from the literature the result for the moment is $\mu[^{59}\mathrm{Cu}]=+1.891(9)\ \mu_N$, which reveals a large deviation from the proton $p_{3/2}$ single-particle value. This provides strong experimental evidence for a massive shell breaking at ^{56}Ni.

DOI: 10.1103/PhysRevC.70.014312 PACS number(s): 21.10.Ky, 21.60.Cs, 29.30.Lw

I. INTRODUCTION

Close to neutron and proton shell closures the structure of odd-*A* nuclei may be well approximated by the single-particle behavior of the particle (hole) outside (inside) the closed shell. The most basic single-particle shell model then predicts the so-called Schmidt values for the nuclear magnetic dipole moments. It is well known that for nuclei farther away from closed shells the magnetic moment differs from the Schmidt value [1]. These deviations are caused by configuration mixing (core polarization) and meson exchange currents (MEC) [2]. The first is related to the fact that the wave functions of the basic shell model assume that the odd nucleon is in a single-particle state, while even small configuration admixtures can already appreciably change the magnetic moment. The second correction takes into account the effects of interaction with the electromagnetic field when two nucleons are interacting.

In case of the odd-*A* Cu isotopes the 29th proton is in the $p_{3/2}$ orbital with a Schmidt moment $\mu_{\mathrm{Schmidt}}=3.79\mu_N$. Below $N=40$, the neutrons occupy the $p_{3/2}$, $f_{5/2}$, and $p_{1/2}$ orbitals. Recently, the development of the RILIS resonance ionization laser ion source [3,4] has allowed the measurement of several new magnetic moments for copper isotopes [5–7] with the ISOLDE facility at CERN. With experimental magnetic moments being available for the odd-*A* isotopes from ^{61}Cu up to ^{69}Cu one can now investigate the neutron number dependence of the moments of the odd-*A* Cu nuclei below $N=40$ and especially towards the $N=28$ shell closure. In this respect the magnetic moment of ^{59}Cu, with 30 neutrons, is of special interest as it paves the way for the measurement of the moment of the $N=28$ isotope ^{57}Cu (^{56}Ni core plus one proton) and at the same time indicates how the systematic trend of odd-Cu moments develops as $N=28$ is approached.

We therefore have measured the magnetic moment of ^{59}Cu at the ISOLDE facility. In addition, shell model calculations were performed using perturbation theory to correct for core polarization and meson exchange currents. Finally, since ^{59}Cu is the mirror nucleus of ^{59}Zn, the decay of which is known, our result can also be compared to the prediction from the correlation between the ground state gyromagnetic ratios and superallowed β-decay transition strengths of the mirror nuclei that was established in Ref. [8].

II. EXPERIMENT

The magnetic moment of ^{59}Cu was measured with the technique of low temperature nuclear orientation (LTNO) [9] combined with nuclear magnetic resonance on oriented nuclei where the destruction of the β asymmetry by the radio frequency signal (β-NMR/ON) was observed with β-particle detectors operating at a temperature of about 10 K inside the NICOLE ^{3}He-^{4}He dilution refrigerator. The combination of these techniques has several advantages for measuring nuclear magnetic moments. Firstly, β asymmetries are significantly larger than γ asymmetries at relatively small values of $\mu B/T$, with μ the nuclear magnetic moment, B the total magnetic field the nuclei experience, and T the sample temperature. Therefore, with β detection even for isotopes with rather small magnetic moments a measurable resonance signal can be obtained at the temperatures accessible with an on-line refrigerator. Secondly, since one can in principle integrate the complete β spectrum the energy resolution of the β detectors is less important. Furthermore, in this experiment the particle (β) detectors were placed inside the 4 K radiation shield of the dilution refrigerator, thereby minimizing scattering or absorption of the β particles on their way to the detectors.

Detailed information on the EC/β^+ decay of ^{59}Cu ($t_{1/2}=81.5$ s, $J^\pi=3/2^-$) can be found in Ref. [10]. The strongest β^+ branch of ^{59}Cu is an allowed $J^\pi=3/2^-\rightarrow J^\pi=3/2^-$ ground state to ground state Gamow-Teller transition with end point energy $E_0=3778$ keV and an intensity of 57.5%. The rest of the β^+ intensity is spread over ten other branches.

*Electronic address: victor.golovko@fys.kuleuven.ac.be

The magnitude of the hyperfine magnetic field of Cu in an iron host lattice is known, but unfortunately not with very high precision: $B_{\mathrm{hf}}=-21.8(1)$ T [5]. In fact, the error of the hyperfine magnetic field will turn out to give the largest contribution to the total error of the nuclear magnetic moment of ^{59}Cu, as will become clear later.

The radioactive ^{59}Cu was produced at ISOLDE (CERN) with a 1.4 GeV proton beam from the Proton Synchrotron Booster, bombarding a ZrO_2 felt target (6.3 g Zr/cm^2) [11] connected to the RILIS [4,7], which provided the required element selectivity for the separation of ^{59}Cu. After ionization and acceleration to 60 keV, the ^{59}Cu beam with an intensity of about 3×10^6 ions/s was mass-separated by the General Purpose Separator, transported through the beam distribution system, and implanted into a polished and annealed 99.99% pure Fe foil (thickness 250 μm) soldered onto the cold finger of the NICOLE ^{3}He-^{4}He dilution refrigerator. The implantation depth of ^{59}Cu ions with an energy of 60 keV is around 200 Å. The corresponding energy loss for the β particles leaving the sample is then of the order of 100 eV, which is negligible in comparison to the β end point energy of ^{59}Cu. The iron foil in which the radioactive ^{59}Cu ions were implanted was magnetized by an external magnetic field generated by a superconducting split-coil magnet. During the measurements a horizontal external magnetic field $B_{\mathrm{applied}}=0.10(2)$ T, produced by the superconducting magnet, was used. Firstly, a field of 0.5 T was applied, in order to magnetically saturate the iron foil. Thereafter, the field was reduced to 0.1 T so as to minimize its influence on the trajectories of the β particles. For the 250 μm thick Fe foil that was used a demagnetization field $B_{dem}=0.0249$ T was calculated. The temperature of the sample was maintained in the region between 10 and 100 mK and measured by a ^{57}CoFe nuclear orientation thermometer [9].

The angular distribution of the positrons emitted during the β^+ decay of ^{59}Cu was observed with three high-purity Ge (HPGe) particle detectors that were installed inside the 4 K thermal shield of the dilution refrigerator. These detectors, with a sensitive diameter of about 12 mm and a thickness of 5 mm were positioned at angles of 15°, 75°, and 165° with respect to the orientation axis defined by the magnetization of the iron foil in the external magnetic field. The thickness of the detectors was chosen such that the end point of the β spectrum could be observed with maximal efficiency while at the same time minimizing the sensitivity to γ rays. Installing these detectors inside the thermal shields means that they have to be able to operate at temperatures close to the temperature of liquid He (i.e., around 10 K). The detectors used were produced and tested in the Nuclear Physics Institute in Řež [12]. Apart from these particle detectors large-volume HPGe detectors for detection of the γ radiation were installed outside the refrigerator.

III. DATA COLLECTION AND ANALYSIS

In order to reduce the search region for the β-NMR/ON measurement, the ^{59}Cu magnetic moment was first determined by scanning the first of the two lasers used to selectively ionize Cu atoms in the RILIS ion source. The on-line analysis of this measurement yielded $|\mu[^{59}\mathrm{Cu}]|=1.90(7)$, corresponding to a resonance frequency $\nu_{res}=209\pm8$ MHz, which determined the search region for the β-NMR/ON experiment. About 200 spectra of 150 s each were recorded. The rf signal was generated by a Marconi generator with a range from 10 kHz to 3.3 GHz. The rf power level was tuned in order to see its effect on the sublevel populations by a small but clear change in the β anisotropy. This anisotropy was defined as the double ratio of the 15° and 165° β-detector count rates at millikelvin temperatures (polarized sample) and at 1 K (unpolarized sample):

$$\frac{W_\beta(15^\circ)}{W_\beta(165^\circ)}=\left[\frac{N(15^\circ)}{N(165^\circ)}\right]_{\mathrm{mK}}\Bigg/\left[\frac{N(15^\circ)}{N(165^\circ)}\right]_{1\ \mathrm{K}}. \quad (1)$$

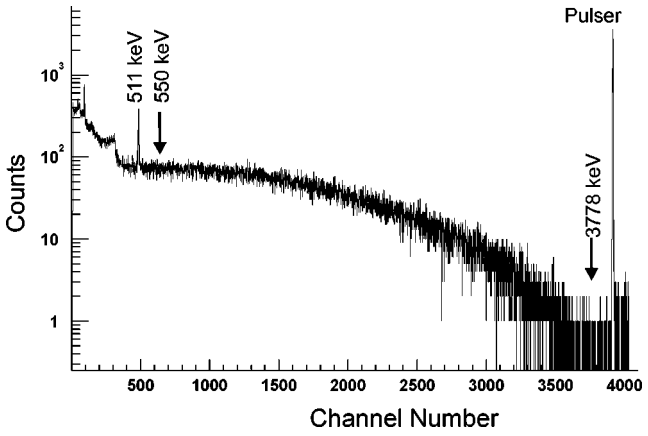

FIG. 1. Typical β spectrum for ^{59}Cu recorded within one 150 s measurement cycle. The 511 keV positron annihilation line and the pulser peak are indicated. For the β-NMR/ON experiment discussed here the spectrum was integrated between 550 keV and 3778 keV (end point).

The resonance experiment was performed at a sample temperature of about 10 mK. Since in a β-NMR/ON experiment one is observing just the destruction of asymmetry in the angular distribution of the β particles through magnetic resonance, we used the complete energy region from 550 keV to 3778 keV in order to increase statistics (Fig. 1). The energy region below 550 keV was not used as it suffered from background of Compton scattered 511 keV γ rays.

At first the frequency was varied from 200 to 220 MHz, both in upward and in downward directions, in 1 MHz steps with 1 MHz modulation amplitude and 0.1 kHz modulation frequency, and sent to the NMR coil that was installed around the cold finger. In these two scans a clear resonance signal was immediately found. Statistics was subsequently improved by three frequency sweeps in upward direction and two sweeps downwards in the region from 203 to 213 MHz. In addition a scan was carried out in the frequency region from 204 to 215 MHz in 0.5 MHz steps with 0.5 MHz modulation amplitude and 0.1 kHz modulation frequency.

The data were corrected for the "dead time" of the data acquisition system using a precision pulse generator. All scans were separately analyzed in order to check for possible systematic errors. No hints for such errors were found. An evaluation of all available data with due regard to relaxation

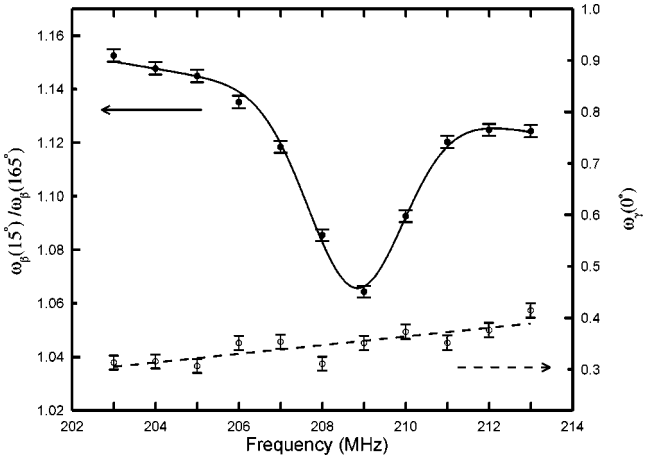

FIG. 2. On-line nuclear magnetic resonance on oriented nuclei curve for ^{59}Cu (sum of five scans: three in upward and two in downward direction). Plotted is the ratio of the pulser normalized count rates for the 15° (L) and 165° (R) β-particle detectors as a function of rf frequency. The integrated destruction of anisotropy is 46%. At the bottom the anisotropy at 0° for the 136 keV γ ray of the ^{57}CoFe thermometer [$W_\gamma(0°)$, corresponding to a sample temperature of about 10 mK] is displayed for the same frequency region, showing no resonant effect at the position of the ^{59}Cu resonance. The slope in the anisotropy versus frequency that is visible for both isotopes is caused by a small heating due to an increase in the power absorption by the system with increasing rf frequency. The amplitude of the signal observed by the pickup coil that was installed around the sample holder indeed increased from 49 mV at 200 MHz to 95 mV at 210 MHz and 210 mV at 220 MHz.

time effects gave for the center frequency the final result $\nu = 208.79(4)$ MHz. To illustrate the quality of the data the resonance curve obtained after summing all scans in the frequency region from 203 to 213 MHz in 1 MHz steps is shown in Fig. 2. The data points were fitted with a straight line in addition to the resonance function to account for the slope in the on-line data. From the resonance frequency, the spin (J) of the ground state of ^{59}Cu, the Planck constant h, and the total magnetic field ($\mathbf{B}_{\rm tot}=\mathbf{B}_{\rm hf}+\mathbf{B}_{\rm applied}-\mathbf{B}_{\rm dem}$), the nuclear magnetic moment of ^{59}Cu is obtained as

$$\mu = \left| \frac{J\ \nu_{\rm res} h}{B_{\rm tot}} \right| \tag{2}$$

yielding

$$\mu[^{59}\mathrm{Cu}] = +1.891(9)\mu_N, \tag{3}$$

where most of the error is due to the uncertainty of the hyperfine field. The center frequency at hyperfine field value is $\nu(B_{ext}=0)=209.51(22)$ MHz. The sign of μ was obtained from the observed β asymmetry and agrees with the systematics for the odd-A $p_{3/2}$ copper isotopes. The difference between our experimental result and the Schmidt value is $\Delta\mu(^{59}\mathrm{Cu})=-1.90(1)$.

IV. SHELL-MODEL RESULTS WITH PERTURBATION THEORY

The copper-isotope ground-state wave functions are characterized by having 28 protons occupying closed-shell orbitals and the 29th proton occupying the $\pi p_{3/2}$ orbital. To start, we consider just ^{57}Cu and ^{69}Cu. In the first case, the neutron number is $N=28$; in the second it is $N=40$. In both these instances the neutrons also may be considered to be occupying closed-shell orbitals. Thus for ^{57}Cu and ^{69}Cu our zeroth-order approximation is to write the ground-state wave function as that of fully occupied closed shells plus a single proton in the $\pi p_{3/2}$ orbital. This zeroth approximation is then corrected in perturbation theory.

Let the Hamiltonian be divided into a one-body Hamiltonian and a residual interaction: $H=H_0+V$, where $H_0=T+U$, the sum of kinetic and one-body potential energy operators, and the residual interaction $V=V_{\rm bare}-U$, where $V_{\rm bare}$ is the two-body potential energy operator. The eigenfunctions of H_0 form the basis of the calculation. For this purpose we will use the harmonic oscillator Hamiltonian. However, one can always add constants to this Hamiltonian that will shift the energy eigenvalues but not change the radial wave functions. Thus we will use the oscillator radial functions in calculating matrix elements, but will use the experimental single-particle energies in calculating energy denominators. For the residual interaction we will use the one-boson exchange potential with a short-range cut-off; more details are given in Ref. [2].

Our requirement is to calculate matrix elements of the one-body magnetic moment operator, to be denoted F. In the zeroth-order approximation, we compute $\langle b|F|a\rangle$, where a and b are single-particle valence states of orbits not in the closed-shell cores. For magnetic moments we need the diagonal matrix element, $a=b$, and for the copper isotopes in particular, $a=b=\pi p_{3/2}$. However, for clarity of displaying the formulas, we will write the initial single-particle state as $|a\rangle$ and the final as $\langle b|$, but take $a=b=\pi p_{3/2}$ when computing the magnetic moment. The correction to the zeroth-order approximation to second order in V is given by [2]

$$\begin{aligned}\langle\psi_b|F|\psi_a\rangle = \langle b|F|a\rangle &+ \sum_\alpha \frac{\langle b|F|\alpha\rangle\langle\alpha|V|a\rangle}{E_a-E_\alpha} + \sum_\alpha \frac{\langle b|V|\alpha\rangle\langle\alpha|F|a\rangle}{E_b-E_\alpha} + \sum_{\alpha,\beta}\langle b|F|\alpha\rangle\frac{\langle\alpha|V|\beta\rangle\langle\beta|V|a\rangle}{(E_a-E_\alpha)(E_a-E_\beta)} - \sum_\alpha\langle b|F|\alpha\rangle\frac{\langle\alpha|V|a\rangle\langle a|V|a\rangle}{(E_a-E_\alpha)^2} \\ &+ \sum_{\alpha,\beta}\frac{\langle b|V|\beta\rangle\langle\beta|V|\alpha\rangle}{(E_b-E_\beta)(E_b-E_\alpha)}\langle\alpha|F|a\rangle - \sum_\alpha\frac{\langle b|V|b\rangle\langle b|V|\alpha\rangle}{(E_b-E_\alpha)^2}\langle\alpha|F|a\rangle + \sum_{\beta,\gamma}\frac{\langle b|V|\beta\rangle}{(E_b-E_\beta)}\langle\beta|F|\gamma\rangle\frac{\langle\gamma|V|a\rangle}{(E_a-E_\gamma)} \\ &- \frac{1}{2}\sum_\beta\langle b|F|a\rangle\frac{\langle a|V|\beta\rangle\langle\beta|V|a\rangle}{(E_a-E_\beta)^2} - \frac{1}{2}\sum_\beta\frac{\langle b|V|\beta\rangle\langle\beta|V|b\rangle}{(E_b-E_\beta)^2}\langle b|F|a\rangle. \end{aligned} \tag{4}$$

TABLE I. Contributions to the calculated effective magnetic moment operator for a $p_{3/2}$ proton in ^{57}Cu and ^{69}Cu. $\Delta\mu$ is the corresponding change in the magnetic moment with respect to the Schmidt value $\mu_{Sch} = 3.79\ \mu_N$.

	^{57}Cu				^{69}Cu			
	δg_l	δg_s	δg_p	$\Delta\mu$	δg_l	δg_s	δg_p	$\Delta\mu$
CP(RPA)	0.007	−1.231	0.344	−0.60	−0.002	−0.981	0.648	−0.47[a]
CP(2nd)	−0.152	−2.034	0.549	−1.15	−0.225	−1.448	0.334	−0.94
MEC	0.116	0.293	−0.058	0.26	0.183	0.368	−0.295	0.36
CP-MEC	0.100	0.259	0.372	0.24	0.103	0.355	0.393	0.30
Isobars	−0.005	−0.142	0.735	−0.05	−0.002	−0.178	0.558	−0.07
Relativistic	−0.024	−0.151	−0.040	−0.10	−0.023	−0.143	−0.038	−0.10
Sum	0.041	−3.004	1.900	−1.39	0.035	−2.027	1.600	−0.92
$\mu_{th} = \mu_{Sch} + \text{sum}$				2.40				2.87

[a]A coding error in the 1999 calculations [5] was corrected here.

Here α stands for a small, finite number of two-particle one-hole, $2p$-$1h$, intermediate states, while β and γ stand for, in principle, an infinite number of $2p$-$1h$ or $3p$-$2h$ states. When F is the magnetic moment operator there are selection rules on $\langle\alpha|F|a\rangle$ that severely limit the number of intermediate states of type α. In particular, they have to be of the structure $|(j_<, j_>^{-1})^{1^+}, a\rangle$ where $j_<$ is a valence orbital with $j = l - \frac{1}{2}$, while $j_>$ is its spin-orbit partner orbital $j = l + \frac{1}{2}$ that is occupied in the closed shells. These orbitals are coupled to angular momentum and parity of 1^+, the multipolarity of the magnetic moment operator. Finally this particle-hole pair is coupled to the valence orbital, a. For the copper isotope, ^{57}Cu, with closed shells at $N=28, Z=28$ there are two states of type α: $|\nu(f_{5/2}, f_{7/2}^{-1}), \pi p_{3/2}\rangle$ and $|\pi(f_{5/2}, f_{7/2}^{-1}), \pi p_{3/2}\rangle$. For ^{69}Cu with closed shells $N=40, Z=28$ the neutron particle-hole state is no longer available so there is only one state of type α, namely $|\pi(f_{5/2}, f_{7/2}^{-1}), \pi p_{3/2}\rangle$. For the states of type β and γ the magnetic moment operator does not provide any restriction on their number, so these summations are in principle infinite. Second-order calculations are therefore computationally quite time consuming even for the magnetic moment operator. For the high-lying intermediate states we approximate their energy by the appropriate multiple of the characteristic oscillator energy, $\hbar\omega$. We explicitly perform the intermediate-state summations up to $12\hbar\omega$, and geometrically extrapolate beyond that.

The terms in Eq. (4) that *only* involve intermediate states of type α—these include the second and third terms contributing in first order and part of the fourth and sixth terms contributing in second order—represent a start of a sequence that can be summed to all orders in perturbation theory. These terms, in fact, yield the random phase approximation (RPA). In Table I we separately identify the results obtained from the RPA terms alone, summed to all orders, as CP(RPA). All the other core-polarization terms summed only to second order are labeled in the table as CP(2nd).

It is convenient to discuss the calculated results in terms of an effective one-body magnetic moment operator:

$$\boldsymbol{\mu}_{\text{eff}} = g_{l,\text{eff}}\mathbf{l} + g_{s,\text{eff}}\mathbf{s} + g_{p,\text{eff}}[Y_2, \mathbf{s}], \tag{5}$$

where $g_{x,\text{eff}} = g_x + \delta g_x$, with $x = l$, s, or p. Here g_x is the single-particle g factor and δg_x the correction to it. For a proton, $g_l = 1.0$, $g_s = 5.587$ and $g_p = 0.0$. Note the presence of an additional term in the effective magnetic moment operator involving a spherical harmonic of rank 2 coupled to the spin operator to give a tensor of multipolarity 1, which is absent in the bare operator. From this decomposition it is evident that the principal impact of the core-polarization terms is to quench the spin g_s factor significantly. This is the major reason for the measured magnetic moments in closed-shell-plus-one nuclei differing from the Schmidt estimates.

Another class of corrections are MEC. We include contributions from π-, ρ-, ω-, and σ-meson exchanges, where σ is a scalar, isoscalar meson, as described in detail in Ref. [2]. In the shell model, MEC are represented by two-body operators denoted here as G. Then the correction to the magnetic moment is given by the expression

$$\langle\psi_b|G|\psi_a\rangle = \langle b|G|a\rangle + \sum_\beta \frac{\langle b|G|\beta\rangle\langle\beta|V|a\rangle}{E_a - E_\beta} + \sum_\beta \frac{\langle b|V|\beta\rangle\langle\beta|G|a\rangle}{E_b - E_\beta}, \tag{6}$$

where as before β stands for, in principle, an infinite number of $2p$-$1h$ or $3p$-$2h$ states. The first term in Eq. (6) we will call the MEC correction and involves the calculation of the matrix element of a two-body operator in single-particle valence states. More explicitly, it is

$$\langle b|G|a\rangle = \sum_h \langle bh|G|ah\rangle, \tag{7}$$

showing that it includes a sum over all the orbitals, h, occupied in the closed-shell cores. The main impact of the MEC correction is to enhance the orbital g_l factor.

The second and third terms in Eq. (6) represent a core-polarization correction to the MEC calculation. It corrects the single valence nucleon description of the copper isotopes to include $2p$-$1h$ and $3p$-$2h$ configurations. Again there are no selection rules to limit the intermediate-state summations,

so as with CP(2nd) we compute the intermediate-state summations up to $12\hbar\omega$ and geometrically extrapolate beyond that. We have labeled this contribution as CP-MEC in Table I. Observe that this core-polarization correction has only been calculated to first order in the residual interaction, V. However since the MEC operator, G, contains meson-nucleon coupling constants to the second power, as does the residual interaction V, this term can be said to be fourth order in meson-nucleon couplings. Similarly the CP(2nd) correction is also fourth order in meson-nucleon couplings. Thus there are many similarities between the CP(2nd) and CP-MEC contributions, but there is one very important difference. The CP-MEC contribution is only first order in perturbation theory and contains only one energy denominator, while CP(2nd) is second order and contains two energy denominators. Since the energy denominator is a negative quantity, this leads to a sign difference between these two contributions. In many ways this is fortunate, since the CP(2nd) contribution is probably the least reliable component in Table I and to have it ameliorated by the CP-MEC contribution is beneficial. In fact, we believe that the sum CP(2nd)+CP-MEC probably cannot be calculated with an accuracy better than, say, 20%. This would be our, somewhat arbitrary, error estimate on the calculated correction to the Schmidt magnetic moment. The other ingredients in Table I can probably be calculated more reliably than this.

Another contribution has been labeled "Isobars" in Table I. This represents the process in which the spin-dependent, isovector component of the residual interaction, principally π and ρ exchange, can excite the nucleon to the Δ-isobar excited state, which then decays in the electromagnetic field. The impact this process has on the magnetic moment can also be represented by a two-body operator, G, so we use Eq. (6) to evaluate its contribution. Since the isobar contribution is quite small, we have not separated the isobar contribution of the first term from its core-polarization correction in the second and third terms. The main impact of the isobars is again to quench the spin g_s factor.

Last, there is a relativistic correction to the single-particle magnetic moment operator. The usually written operator, $g_l\mathbf{l}+g_s\mathbf{s}$, is the lowest order term in a nonrelativistic reduction of the electromagnetic current. If the next order in p^2/M^2, where p is a typical nucleon momentum and M its mass, is retained the magnetic moment operator is [2]

$$g_l\left\{\mathbf{l}\left(1-\frac{p^2}{2M^2}\right)-\left(\frac{p^2}{2M^2}\right)(\mathbf{s}-(\mathbf{s}\cdot\hat{\mathbf{p}})\hat{\mathbf{p}})\right\}+g_s\mathbf{s}\left(1-\frac{p^2}{2M^2}\right). \tag{8}$$

In terms of the effective magnetic moment operator defined in Eq. (5), we identify

$$\delta g_l=-\frac{1}{2}g_l\left\langle\frac{p^2}{2M^2}\right\rangle \quad \delta g_s=\left(-\frac{1}{3}g_l-\frac{1}{2}g_s\right)\left\langle\frac{p^2}{2M^2}\right\rangle$$

$$\delta g_p=-\frac{1}{6}(8\pi)^{1/2}g_l\left\langle\frac{p^2}{2M^2}\right\rangle. \tag{9}$$

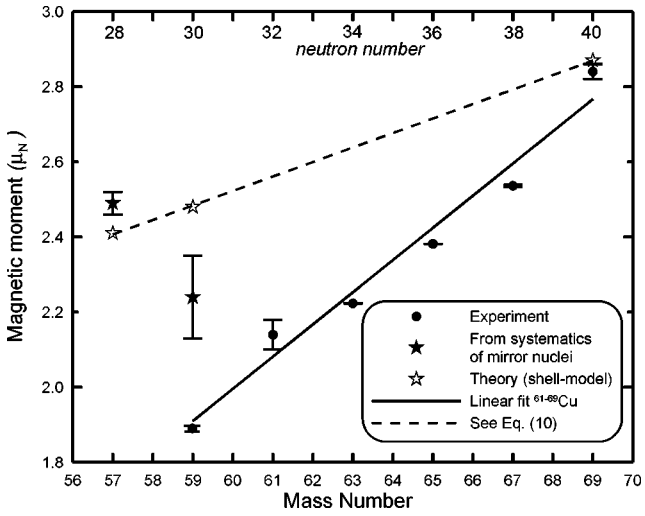

FIG. 3. Experimental magnetic moments for the odd-A $^{59-69}$Cu isotopes (*black dots*) (Refs. [5,6,13] and this work), shell model predictions for ^{57,59}Cu (*open stars*) (see Sec. IV), and predictions for ^{57,59}Cu based on systematics of the mirror nuclei [8] (*black stars*). The prediction for ^{59}Cu from a linear fit (*full line*) to the experimental values for $^{61-69}$Cu is shown as well.

It remains to estimate the expectation value $\langle p^2/2M^2\rangle \equiv \langle a|p^2/2M^2|a\rangle$ for which we use harmonic oscillator wave functions. Although this correction is sensitive to the choice of radial wave function, because it depends on its second derivative, the correction is quite small, about 3% of the Schmidt value, so the choice of the radial function ultimately is not critical.

All the calculated corrections are collated in Table I. For the $p_{3/2}$ proton in ^{69}Cu, the calculated correction to the single-particle magnetic moment is $\Delta\mu(^{69}\text{Cu})=-0.91\mu_N$, in good agreement with the experimental value [5] of $-0.95(1)\mu_N$. For ^{57}Cu, the calculated correction is $\Delta\mu(^{57}\text{Cu})=-1.39\mu_N$, where the error on the calculation, as mentioned, has been arbitrarily set at 20% of the CP(2nd)+CP-MEC value. There is no experimental measurement for ^{57}Cu, but it is clear from Fig. 3 that any reasonable extrapolation from the known data on the odd-mass copper isotopes will produce a result significantly different from this calculated value.

The isotope ^{59}Cu has two valence neutrons outside the $N=28$ closed shells as well as the $p_{3/2}$ proton. So we have to estimate the impact of these two extra valence neutrons on the calculation of the magnetic moment. The difference between the two calculations given in Table I is that in ^{57}Cu the neutron orbits $1p_{3/2}$, $0f_{5/2}$, $1p_{1/2}$ are empty, while at ^{69}Cu they are taken to be full. This impacts on the calculation of the core-polarization and meson-exchange corrections in that in the sums over intermediate states α, β, γ in Eqs. (4) and (6) these neutron orbits are part of the sum over particle orbits for ^{57}Cu, but part of the sum over hole orbits for ^{69}Cu. This effect alone is responsible for most of the difference between $\Delta\mu(^{57}\text{Cu})$ and $\Delta\mu(^{69}\text{Cu})$. If we make the reasonable assumption that the contribution of these neutron orbitals for the odd-mass copper isotopes lying between these two ex-

TABLE II. Experimental and theoretically calculated magnetic moments (in units of nuclear magneton μ_N) for odd-A copper-isotopes in the $N \approx Z$ region.

A	N	μ_{th}[a]	μ_{mir}[b]	μ_{fit}	μ_{exp}[c]
57	28	2.40	2.49(3)		
59	30	2.48	2.24(11)	1.91[d]	+1.891(9)[e]
61	32				+2.14(4)
63	34				+2.22329(18)
					2.2272057(31)
					2.2273456(14)
65	36				+2.38167(25)
					2.38161(19)
67	38				+2.54(2)[f]
69	40	2.87			+2.84(1)[g]

[a]Theoretical predictions from the shell-model; see Sec. IV.
[b]Predictions from systematics of mirror nuclei [8].
[c]From the Table of Nuclear Moments [13].
[d]Extrapolation based on a straight line fit to the experimental data for $^{61-69}$Cu.
[e]This work.
[f]From Ref. [6].
[g]From Ref. [5].

tremes is proportional to the neutron population, then we can get an estimate for the change $\Delta\mu(^{59}\text{Cu})$ of the magnetic moment with respect to the Schmidt value as

$$\Delta\mu(^{59}\text{Cu}) = \Delta\mu(^{57}\text{Cu}) + \frac{2}{12}[\Delta\mu(^{69}\text{Cu}) - \Delta\mu(^{57}\text{Cu})] = -1.31\mu_N, \quad (10)$$

corresponding to $\mu_{th}(^{59}\text{Cu}) = 2.48\mu_N$.

V. DISCUSSION AND CONCLUSION

Table II and Fig. 3 summarize all presently available experimental magnetic moments for the odd-A copper isotopes, as well as the results from the shell model calculations described in the previous section and predictions for the moments of ^{57,59}Cu deduced from the correlation between the ground state gyromagnetic ratios and superallowed β-decay transition strengths of the mirror nuclei established in Ref. [8]. Also listed is the extrapolated value obtained from fitting a straight line to the available experimental data for $^{61-69}$Cu.

The estimate $\mu(^{59}\text{Cu}) = 2.48\mu_N$ that is obtained from the shell model calculations stands at considerable distance from the experimental value of $+1.891(9)\mu_N$. It is doubtful, however, that a shell-model calculation based on a $N=28$ closed-shell core will produce a result significantly different from Eq. (10). The real problem is that the calculated magnetic moment in the closed-shell-plus-one nucleus ^{57}Cu stands so far from the extrapolation of known data on odd-mass copper isotopes shown in Fig. 3. Indeed, fitting a straight line through the experimental magnetic moment values for the $3/2^-$ odd-mass ^{61}Cu to ^{69}Cu isotopes yields $\mu(^{59}\text{Cu}) = 1.91\mu_N$.

In the calculation described in the previous section, it is implicitly assumed that ^{56}Ni is principally a doubly closed-shell nucleus and any departure from this can be estimated in perturbation theory. In this scheme, the breaking of the closed shells is quite modest. On the other hand, there is significant evidence mainly from large-scale shell-model calculations [14–16] that there is a massive amount of shell breaking at ^{56}Ni. If this is the case, then the starting hypothesis of our calculations is poor, and hence the poor result in the comparison of theory with experiment for the ^{59}Cu magnetic moment. Indeed, we could reverse this argument by stating that the measured magnetic moment for ^{59}Cu provides further evidence of the massive shell-breaking at ^{56}Ni. Further, since the measured and calculated magnetic moments for ^{69}Cu are in good agreement with each other, one could even argue that ^{68}Ni, with $N=40$, is a better doubly magic closed-shell nucleus than ^{56}Ni. In view of this a measurement of the magnetic moment of the "closed-shell-plus-one" nucleus ^{57}Cu now becomes even more important. Such a measurement is actually being planned [17].

Of note is a recent study of $f_{7/2}$ valence states in nuclei with $A<56$ by Speidel *et al.* [18]. These authors carry out both perturbation-theory calculations and shell-model diagonalizations in examining the systematic behavior of the magnetic moment g factor over a sequence of nuclei. Their results showed a surprising sensitivity to the choice of effective interaction. This is traced to the key matrix element $\langle f_{7/2}f_{7/2}|V|f_{7/2}f_{5/2}\rangle_{I=2,T=1}$ being ill determined. For example, in the Kuo-Brown interaction [19] this matrix element is obtained from a bare G matrix and a core-polarization correction as $G+G_{3p\text{-}1h} = -0.124 + 0.124 = 0$ MeV. This strong cancellation, therefore, explains why this matrix element is ill determined. In our study of $p_{3/2}$ valence states in copper isotopes, our key matrix elements contributing to the CP(RPA) correction are $\langle \pi p_{3/2}^{-1}\pi p_{3/2}|V|\nu f_{7/2}^{-1}\nu f_{5/2}\rangle_{J=1}$ and $\langle \pi p_{3/2}^{-1}\pi p_{3/2}|V|\pi f_{7/2}^{-1}\pi f_{5/2}\rangle_{J=1}$. Both contribute to the calculation of ^{57}Cu, but only the latter to ^{69}Cu. With the Kuo-Brown interaction, these matrix elements are $G+G_{3p\text{-}1h} = -0.421 + 0.070 = -0.352$, and $G+G_{3p\text{-}1h} = -0.904 - 0.061 = -0.965$ MeV, respectively. In these cases the $G_{3p\text{-}1h}$ terms give only a modest correction, so we expect the dependence on the effective interaction to be less dramatic in our study. Nevertheless, if an effective interaction can be found that strengthens the first particle-hole matrix element, while leaving the second unaltered, then this would lead to an improvement in the theoretical understanding of the magnetic moment data.

Finally, our result can also be compared to the prediction which Buck *et al.* [8] recently obtained from the linear relation they deduced between the ground state g factors and the superallowed β-decay strength of mirror nuclei

$$\mu_{mir}(^{59}\text{Cu}) = 2.24(11)\mu_N. \quad (11)$$

Clearly, this prediction is not in very good agreement with the experimental value either. It is based on the experimental log $ft=3.69(2)$ for the mirror isotope ^{59}Zn. Inserting our experimental value for the magnetic moment of ^{59}Cu in the relations deduced in Ref. [8] yields log $ft(^{59}\mathrm{Zn})=-3.75(1)$, which differs slightly from the experimental value, and in addition provides a new prediction for the magnetic moment of the mirror isotope ^{59}Zn, i.e., $\mu_{mir}(^{59}\mathrm{Zn})=-0.28(2)\mu_N$.

ACKNOWLEDGMENTS

We are very grateful to V. Fedoseyev and D. Fedorov for the operation of the RILIS ion source. This work was supported by the Fund for Scientific Research Flanders (FWO), the IHRP program of the European Commission (Contract No. HPRI-CT-1999-00018), and the Grant Agency of the Czech Republic.

[1] A. Bohr and B. R. Mottelson, *Nuclear Structure* (World Scientific, Singapore, 1998), Vol. 1.
[2] I. S. Towner, Phys. Rep. **155**, 263 (1987).
[3] Y. Kudryavtsev *et al.*, Nucl. Instrum. Methods Phys. Res. B **114**, 350 (1996).
[4] U. Köster *et al.*, Nucl. Instrum. Methods Phys. Res. B **160**, 528 (2000).
[5] J. Rikovska *et al.*, Phys. Rev. Lett. **85**, 1392 (2000).
[6] J. Rikovska and N. J. Stone, Hyperfine Interact. **129**, 131 (2000).
[7] L. Weissman *et al.*, Phys. Rev. C **65**, 024315 (2002).
[8] B. Buck, A. C. Merchant, and S. M. Perez, Phys. Rev. C **63**, 037301 (2001).
[9] *Low-Temperature Nuclear Orientation*, edited by H. Postma and N. J. Stone (Elsevier, Amsterdam, 1986).
[10] *Table of Isotopes*, edited by R. B. Firestone (Wiley, New York, 1996), Vol. 1.
[11] U. Köster *et al.*, Nucl. Instrum. Methods Phys. Res. B **204**, 303 (2003).
[12] D. Vénos, A. Van Assche-Van Geert, N. Severijns, D. Srnka, and D. Zákoucký, Nucl. Instrum. Methods Phys. Res. A **454**, 403 (2000).
[13] P. Raghavan, At. Data Nucl. Data Tables **42**, 189 (1989).
[14] T. Otsuka, M. Honma, and T. Mizusaki, Phys. Rev. Lett. **81**, 1588 (1998).
[15] M. Honma, B. A. Brown, T. Mizusaki, and T. Otsuka, Nucl. Phys. **A704**, 134c (2002).
[16] A. F. Lisetskiy, N. Pietralla, M. Honma, A. Schmidt, I. Schneider, A. Gade, P. von Brentano, T. Otsuka, T. Mizusaki, and B. A. Brown, Phys. Rev. C **68**, 034316 (2003).
[17] T. Mertzimekis *et al.*, NSCL experiment No. 02004, PAC 26, 2003.
[18] K.-H. Speidel, R. Ernst, O. Kenn, J. Gerber, P. Maier-Komar, N. Benczer-Koller, G. Kumbartzi, L. Zamick, M. S. Fayache, and Y. Y. Sharon, Phys. Rev. C **62**, 031301(R) (2000).
[19] T. T. S. Kuo and G. E. Brown, Nucl. Phys. **A114**, 241 (1968).